

The spin-forbidden reaction $\text{CH}({}^2\Pi) + \text{N}_2 \rightarrow \text{HCN} + \text{N}({}^4\text{S})$ revisited.

II. Nonadiabatic transition state theory and application

Qiang Cui, Keiji Morokuma, and Joel M. Bowman

Cherry L. Emerson Center for Scientific Computation and Department of Chemistry, Emory University, Atlanta, Georgia 30322

Stephen J. Klippenstein

Department of Chemistry, Case Western Reserve University, Cleveland, Ohio 44106-7078

(Received 22 May 1998; accepted 24 February 1999)

Transition state theory is extended straightforwardly to treat nonadiabatic processes and applied to study the rate constant of the spin-forbidden reaction $\text{CH}({}^2\Pi) + \text{N}_2 \rightarrow \text{HCN} + \text{N}({}^4\text{S})$. A one-dimensional model was set up to calculate the intersystem crossing probability with the distorted wave approximation and using an *ab initio* value of the spin-orbit coupling. The effect of orthogonal degrees of freedom was then considered by energy convolution with the vibrational frequencies, obtained from *ab initio* calculations, orthogonal to the crossing seam at the minimum of the seam of crossing (MSX), also obtained from *ab initio* calculations. An expression for the cumulative reaction probability, $N(E)$, of the reaction was obtained by a straightforward extension of the unified statistical theory, where the MSX was treated as a transition state. The calculated thermal rate constant, $k(T)$, seems to be too low by two orders of magnitude compared to experimental measurements and an empirical transition state study where *empirical* vibrational frequencies at the MSX are lower by a factor of 2 than those derived here. The disagreement strongly suggests that the current treatment of the multidimensional dynamics needs to be improved. In particular, it may be a poor assumption that spin-forbidden transition takes place with uniform probability on the seam in the case we are considering. © 1999 American Institute of Physics. [S0021-9606(99)02419-8]

I. INTRODUCTION

The calculation of the rate constant of a multistep chemical reaction has been a long-standing issue in physical chemistry, which can be solved at levels of different sophistication. The simplest expression of chemical reaction rate can be derived by invoking the assumption of statistical distribution of energy in the internal degrees of freedom in a molecule. With this fundamental assumption along with separable Hamiltonian, textbook derivations lead to the well-known transition state theory (TST),¹ which in the particular case of unimolecular reaction process is equivalent to the RRKM (Rice–Ramsperger–Kassel–Marcus) theory.² Due to its simplicity, the RRKM theory has been widely used in the kinetic modeling of a wide range of chemical reactions, and recently much attention has been paid to barrierless processes such as radical recombination.³ There has also been tremendous progress in the methodology of calculating canonical or microcanonical rate constants “directly and correctly” from rigorous quantum mechanics, within a time-independent⁴ or time-dependent⁵ framework. However, such kinds of calculations are still restricted to small molecules with only a few active degrees of freedom.

For nonadiabatic chemical processes, it is even more difficult to carry out a rigorous quantum mechanical calculation for the rate constant. The methodology is not very different from that for adiabatic reactions, which actually has been extended to nonadiabatic process with model potentials.⁶ The

main difficulty lies in the fact that a tremendous effort has to be paid to construct two or more potential energy surfaces (PESs) and also to calculate the coupling elements between them. It would be very useful to have an expression for the nonadiabatic reaction rate constant, which is as simple as the standard TST and can be applied to a realistic system with limited information required. Not surprisingly, such an idea is not entirely new, and has been discussed by a few authors in different contexts.⁷ Among those, the studies of Lorquet *et al.*^{7(a)} are the closest to our treatment. However, little work has been carried out using potential energy parameters derived directly from rigorous *ab initio* treatment of the seam of crossing between electronic states. Bearing this in mind, we have made a rather straightforward extension of the standard TST expression to treat nonadiabatic processes. The detailed derivation will be presented in Sec. II, and an application of the theory to a fundamental combustion reaction $\text{CH}({}^2\Pi) + \text{N}_2 \rightarrow \text{HCN} + \text{N}({}^4\text{S})$ will be presented in Sec. III. The parameters required in the rate constant calculations are derived from high level *ab initio* work, which has been presented in a separate paper.⁸ Finally in Sec. IV, we draw a few conclusions.⁹

II. THEORY—EXTENSION OF TST TO NONADIABATIC CHEMICAL REACTIONS

In this section, we first briefly review the rate theories for adiabatic reactions, and then we shall see that the gener-

alization to nonadiabatic processes emerges naturally. Finally, some considerations of practical implementations conclude this section.

A. Standard transition state rate theory for adiabatic processes

As is well established, the central quantity in the rate constant calculation is the cumulative reaction probability (CRP) $N(E)$ for the total energy E , which within the framework of classical mechanics is defined as the following:¹⁰

$$N(E) = 2\pi\hbar(2\pi\hbar)^{-F} \int d\mathbf{p} \int d\mathbf{q} \times \delta[E - H(\mathbf{p}, \mathbf{q})] F(\mathbf{p}, \mathbf{q}) \chi(\mathbf{p}, \mathbf{q}), \quad (1)$$

where $H(\mathbf{p}, \mathbf{q})$ is the classical Hamiltonian of the F -dimensional molecular system. The flux operator $F(\mathbf{p}, \mathbf{q})$ is defined at a dividing surface f , which in most cases is a function of the coordinate expressed as $f(\mathbf{q})=0$, although in general it can also depend on the momentum.¹¹ For a given dividing surface, the flux operator is then expressed as the following:

$$F(\mathbf{p}, \mathbf{q}) = \frac{d}{dt} h(f(\mathbf{q})) = \delta(f(\mathbf{q})) \frac{\partial f}{\partial \mathbf{q}} \cdot \mathbf{p}/m. \quad (2)$$

The last important quantity in Eq. (1) is the characteristic function, which by definition is the following expression:

$$\chi(\mathbf{p}, \mathbf{q}) = \lim_{t \rightarrow \infty} h(f(\mathbf{q}(t))). \quad (3)$$

A rigorous calculation of $N(E)$ requires explicit dynamical simulations, since the long time limit of trajectories has to be monitored as indicated in Eq. (3). In the standard TST, as an approximation, one replaces the characteristic function, which contains all the dynamical information of the system, by a Heaviside step function in terms of the momentum perpendicular to the dividing surface:

$$\chi_{\text{TST}}(\mathbf{p}, \mathbf{q}) = h \left[\frac{\partial f(\mathbf{q})}{\partial \mathbf{q}} \cdot \mathbf{p}/m \right]. \quad (4)$$

As is well documented, such a ‘‘no-recrossing’’ approximation makes TST rigorously the upper bound for the exact classical rate constant, which forms the basis of varieties of *variational* transition state theories.¹²

In most cases, a planar dividing surface $f(\mathbf{q})=q_F=0$ across the saddle point or the transition state (TS) at the reaction coordinate value of $q_F=0$ is used and the $N(E)$ can be simplified as the following:

$$N_{\text{TST}}(E) = 2\pi\hbar(2\pi\hbar)^{-F} \int d\mathbf{p} \int d\mathbf{q} \delta[E - H] \times \delta(q_F) p_F / m h(p_F) = (2\pi\hbar)^{-(F-1)} \int d\mathbf{p}' \int d\mathbf{q}' h[E - H^\ddagger(\mathbf{p}', \mathbf{q}')], \quad (5)$$

where $(\mathbf{p}', \mathbf{q}')$ indicates that reaction coordinate and its conjugate momentum, (p_F, q_F) , have been integrated out, and

$$H^\ddagger = \sum_{k=1}^{F-1} \frac{p_k^2}{2m} + V(\mathbf{q}', q_F=0).$$

As discussed by Miller, the usual TST expression of $k(T)$ can be obtained from Eq. (5) if the further assumption of separable Hamiltonian for the molecular system is invoked. Quantum mechanically, the phase space integral in Eq. (5) is equivalent to the number of rovibrational states, which can be obtained efficiently via the direct counting procedure,¹³

$$N_{\text{TST}}^{\text{HO}} = \sum_{\{n\}} h[E - \epsilon_{\{n\}}^\ddagger], \quad (6)$$

where $\{n\}$ denotes collection of quantized rovibrational states.

It was also pointed out by Miller that by assuming the inverse parabolic potential for the reaction coordinate, a simple Wigner-tunneling corrected rate expression can be obtained:

$$N_{\text{TST}}^{\text{HO/tunnel}} = \sum_{\{n\}} P_{\text{Wigner}}[E - \epsilon_{\{n\}}^\ddagger], \quad (7)$$

where the Heaviside function in Eq. (6) is simply replaced by the Wigner tunneling coefficient across a parabolic barrier. A similar expression has also been derived by Bowman, where the reaction probability is obtained in a general reduced dimensionality space.¹⁴

B. Extension to nonadiabatic process

One may distinguish two general types of nonadiabatic processes, those induced by weak electronic coupling elements such as spin-orbit interaction (case I), and those induced by derivative coupling.¹⁵ One may further divide the latter into cases involving electronic states of different spatial symmetries (case IIA), and those involving electronic states of the same spatial symmetries (case IIB). For case I, the coupling element is clearly defined at least in a perturbational sense,¹⁶ and most important, a one-dimensional reaction coordinate can usually be defined to describe the transition process. These are not necessarily true in general for case IIA or case IIB nonadiabatic processes. In the current work, we shall mainly consider the relatively simpler case I and only briefly discuss the possibility of extending the theory further to cases IIA and IIB.

It is seen from Sec. II A that to calculate the $N(E)$ within a TST framework, one has to obtain the following quantities: (i) the definition of the dividing surface, (ii) the reaction coordinate, (iii) the Hamiltonian in terms of the reaction coordinate and those coordinates orthogonal to it, and (iv) the characteristic function. In the following, we shall discuss these quantities for a general non-adiabatic reaction.

(i) *Expression of the dividing surface.* In the standard TST, one uses the hyperplane which is perpendicular to the reaction coordinate and contains the saddle point: $q_F=0$. For nonadiabatic reactions, one usually treats the MSX (minimum on the seam of crossing) between the two PESs involved as the transition state, although it is not a stationary point on either of them. In addition, to conserve energy and momentum classically, the molecule can only make transition on the seam surface where the two states are degenerate. Therefore, it is natural to choose the seam of crossing as the dividing surface. The obvious difficulty with such a dividing surface is that no general analytical expression exists for it. Thompson *et al.*^{7(b)} circumvented the problem by a Monte Carlo sampling scheme so that the seam is generated numerically “on the fly,” which may not be practical for polyatomic cases. In the work of Lorquet *et al.*,^{7(a)} a “reaction coordinate” x is picked rather arbitrarily and the dividing surface is just taken as the hyperplane that is perpendicular to x and contains the crossing point. In the current work, we solve the problem by using a simple Taylor series expansion of the two PESs around the MSX.

Let us start by recalling the definition and a few geometrical properties of MSX and the seam of crossing. Let $V_1(\mathbf{q})$ and $V_2(\mathbf{q})$ be the two PESs in the problem belonging to case **I**, which behave like the diabatic states in the usual sense due to their different symmetries (spatial \times spin). The \mathbf{q} is the mass-weighted Cartesian coordinate vector, where the mass factor is not essential for general description of the seam but is convenient in the normal model analysis we shall discuss later. The seam surface can be defined with the simple condition:

$$V_1(\mathbf{q}) - V_2(\mathbf{q}) = 0. \quad (8)$$

Expanding both $V_1(\mathbf{q})$ and $V_2(\mathbf{q})$ up to the first order in terms of the gradient vectors $g_i(\mathbf{q})$, we may write, in the vicinity of the seam:

$$[V_1(\mathbf{q}_0) - V_2(\mathbf{q}_0)] + \Delta q \cdot [g_1(\mathbf{q}) - g_2(\mathbf{q})]_{\mathbf{q}_0} = 0. \quad (9)$$

Clearly, the norm of the seam surface is nothing but the normalized energy difference gradient,

$$\hat{\mathbf{s}} = \frac{g_1(\mathbf{q}) - g_2(\mathbf{q})}{|g_1(\mathbf{q}) - g_2(\mathbf{q})|} \Big|_{\mathbf{q}_0}.$$

In the following, $\hat{\mathbf{s}}$ is used to denote the normalized vector, and s is used to denote the numerical value of the displacement along $\hat{\mathbf{s}}$.

The MSX is defined by the two following conditions:

$$V_1(\mathbf{q}) - V_2(\mathbf{q}) = 0 \Leftrightarrow V_1 \text{ and } V_2 \text{ are degenerate,} \quad (10a)$$

$$(\hat{\mathbf{I}} - \hat{\mathbf{s}}\hat{\mathbf{s}})g_i(\mathbf{q}) = \hat{\mathbf{0}} \Leftrightarrow \text{minimum on the seam of crossing.} \quad (10b)$$

As discussed by many authors including us, it is straightforward to set up a Newton–Raphson optimization scheme to

locate the MSX with these two constraints.^{15,17,18} Since MSX is a true minimum *on the seam of crossing*, it is valid to make harmonic expansion of the potential energy around the MSX on the seam of crossing. Following the seminal paper of Miller *et al.* on the reaction path Hamiltonian,¹⁹ one can achieve this by diagonalizing a projected Hessian matrix:

$$\mathbf{H}' = (\hat{\mathbf{I}} - \hat{\mathbf{P}})\mathbf{H}(\hat{\mathbf{I}} - \hat{\mathbf{P}}), \quad (11)$$

where the projector $\hat{\mathbf{P}}$ contains the normal vectors corresponding to the infinitesimal total translation, rotation, and the energy difference gradient vector $\hat{\mathbf{s}}$,

$$\hat{\mathbf{P}} = \sum_{\lambda=1}^3 \mathbf{L}_{\lambda}^{\text{Tr}} \mathbf{L}_{\lambda}^{\text{Tr}} + \sum_{\lambda=1}^3 \mathbf{L}_{\lambda}^{\text{Rot}} \mathbf{L}_{\lambda}^{\text{Rot}} + \hat{\mathbf{s}}\hat{\mathbf{s}}, \quad (12)$$

where the $\mathbf{L}_{\lambda}^{\text{Tr}}$, $\mathbf{L}_{\lambda}^{\text{Rot}}$ are given as the following:

$$\mathbf{L}_{i\gamma,\lambda}^{\text{Tr}} = \sqrt{m_i/M} \delta_{\gamma,\lambda}, \quad (13a)$$

$$\mathbf{L}_{i\gamma,\lambda}^{\text{Rot}} = \sum_{\alpha\beta} (\mathbf{I}_0)_{\lambda\alpha}^{-1/2} \sqrt{m_i} (\mathbf{r}_i - \mathbf{r}_0)_{\beta} \epsilon_{\alpha\beta\gamma}. \quad (13b)$$

It is interesting to point out that *at* the MSX the gradient vectors of the two electronic states are either parallel or antiparallel.²⁰ Therefore the $\hat{\mathbf{s}}$ vector is parallel or antiparallel to the gradient of each PES, and the projector in Eq. (12) becomes exactly the same as that in the case of reaction path Hamiltonian. Therefore, one can directly calculate the projected vibrational frequencies at the MSX with any *ab initio* package that can handle reaction path frequency calculations, such as GAMESS²¹ and GAUSSIAN94²² (although we have independently written a program to carry out projected vibrational frequency calculations and confirmed the results obtained with GAUSSIAN94 in the case of CHN₂). As discussed in paper I of the series, the degeneracy condition (10) is up to first order and the error starts from the second order, which implies that the projected vibrational frequencies for the two electronic states involved will not be exactly the same.⁸

From the normal mode analysis at MSX, one obtains $(3N-7)$ nonzero eigenvalues corresponding to the bound motion on the seam surface, and 7 zero eigenvalues (except for numerical error) corresponding to the total translation/rotation and the norm of the seam surface. According to the eigenvectors, one also obtains a new set of orthonormal coordinates $\{\mathbf{Q}\}$, which are also orthogonal to $\hat{\mathbf{s}}$. With this new set of coordinates, the two diabatic potentials can then be expressed as:

$$V_i(\mathbf{q}) \equiv V_i(s, \mathbf{Q}) = V_i(s) + \frac{1}{2} \sum_k \omega_{ik}^2(0) Q_k^2(0) \quad (14)$$

and the dividing surface can be expressed by the simple equation:

$$s = (\mathbf{q} - \mathbf{q}_0) \cdot \hat{\mathbf{s}} = 0. \quad (15)$$

One may notice the apparent similarity between Eq. (14) and the expression in the reaction path Hamiltonian theory. However, there is a very fundamental difference between the two. In the case of reaction path Hamiltonian theory, one can, in principle, carry out the normal mode analysis at any value of s , including trivially the saddle point ($s=0$). In the current case of surface crossing, on the other hand, the normal mode analysis is valid only at the MSX where $s=0$, since the two electronic states are no longer degenerate if there is displacement along $\hat{\mathbf{s}}$, at least in the first-order sense.

The current expression of the seam surface is by no means exact, because as soon as one steps far from the MSX, the norm of the seam might change. However, the current choice is definitely well defined for a general polyatomic system. With the current description of the seam, the normal mode analysis is also uniquely defined. The fact that transition in most cases takes place in a very restricted area on the PES also makes the $\{\hat{\mathbf{s}}, \mathbf{Q}\}$ representation sufficient to describe the hopping process.

(ii) *The ‘‘hopping’’ coordinate.* As discussed previously, we have made an orthogonal coordinate transformation from the mass-weighted Cartesian $\{\mathbf{q}\}$ to $\{\hat{\mathbf{s}}, \mathbf{Q}\}$. We should emphasize that in most realistic reactions, the ‘‘hopping’’ coordinate is *not* the coordinate that leads to the products. Therefore, the $N(E)$ one calculates at the MSX may only be a component in the total CRP. One usually has to consider the reaction as a multistep process, and derive the rate constant for the whole reaction with the $N(E)$'s calculated at several critical structures. The reaction of $\text{CH} + \text{N}_2$ is a very typical example, as we shall discuss in Sec. III.

(iii) *System Hamiltonian.* After the normal mode analysis, the potential of each diabatic state on the seam can be expressed as in Eq. (14) with $s=0$. The next task is to find the conjugate momenta in the new coordinate $\{\hat{\mathbf{s}}, \mathbf{Q}\}$ and therefore express the kinetic energy operator. In the case of the reaction path Hamiltonian, Miller *et al.* considered the change of the normal modes orthogonal to the path as a function of s , therefore the final kinetic energy expression is quite complicated and contains the curvature terms which represents the coupling between the reaction coordinate and the modes orthogonal to it.¹⁹ In the current case, we can carry out the coordinate transformation rigorously only at the MSX. Therefore the kinetic operators are much simpler than for $s \neq 0$,

$$P_s = \sum_{i=1}^F p_i \hat{\mathbf{s}}_i, \quad (16a)$$

$$P_k = \sum_{i=1}^F p_i L_{i,k}, \quad k=1, \dots, F-1, \quad (16b)$$

where the lower case p_i are Cartesian momenta. The system Hamiltonian can then be expressed as (without translation/rotation):

$$H_i = \frac{P_s^2}{2} + V_i(s) + \sum_k \left[\frac{P_k^2}{2} + \frac{1}{2} \omega_k^2 Q_k^2 \right]. \quad (17)$$

With the expressions of the dividing surface, the ‘‘hopping’’ coordinate, and the system Hamiltonian, the TST expression for $N(E)$ for a nonadiabatic process can be written according to Eqs. (1) and (2) as the following:

$$\begin{aligned} N(E) &= 2\pi\hbar(2\pi\hbar)^{-F} \int d\mathbf{p} \int d\mathbf{q} \\ &\quad \times \delta[E - H(\mathbf{p}, \mathbf{q})] F(\mathbf{p}, \mathbf{q}) \chi(\mathbf{p}, \mathbf{q}) \\ &= (2\pi\hbar)^{-(F-1)} \int dp_s \int ds \int d\mathbf{p}_Q \int d\mathbf{Q} \mathbf{J} \\ &\quad \times \delta[E - H^{F-1}(\mathbf{p}_Q, \mathbf{Q}) - h(p_s, s)] \\ &\quad \times \delta(s) p_s \chi(p_s, Q), \end{aligned} \quad (18)$$

where the Jacobian factor is 1 due to the orthogonal nature of the coordinate transformation $\{\mathbf{q}\} \rightarrow \{\mathbf{s}, \mathbf{Q}\}$. To further carry out the integration in Eq. (18), one needs to specify the characteristic function which will be discussed in the following.

(iv) *The characteristic function.* The characteristic function for a nonadiabatic process is clearly just a probability factor that the system makes transition from one to the other diabatic surface,

$$\chi(\sqrt{2E_s}, Q) = P_{\text{tr}}(\sqrt{2E_s}, Q). \quad (18a)$$

In the standard TST, all the trajectories with momenta pointing toward products are counted in the rate expression. In the nonadiabatic process, the trajectory with momenta pointing toward the reactants can also make diabatic transitions and contribute to the rate constant. Therefore, in the weak coupling limit, no Heaviside function of the momentum appears in Eq. (18a). In the stronger coupling regime, the reverse flux has to be weighted as suggested by Thompson *et al.*⁷

Carrying out the integration over s and p_s in Eq. (18), one obtains the following:

$$\begin{aligned} N(E) &= 2 \times (2\pi\hbar)^{-(F-1)} \int d\mathbf{p}_Q \int d\mathbf{Q} \\ &\quad \times h[E - H^{F-1}(\mathbf{p}_Q, \mathbf{Q})] \chi(\sqrt{2E_s}, Q), \end{aligned} \quad (19)$$

where the characteristic function depends in general on the energy in the \mathbf{s} degree of freedom $E_s = E - H^{F-1}$, and also on \mathbf{Q} . The factor 2 comes from the fact that flux of both $+s$ and $-s$ directions can contribute to the rate constant.

The evaluation of the phase space integral in Eq. (19) can be rather complicated if one considers the transition probability as a function of \mathbf{Q} coordinates. A great simplification can be achieved if the transition probability is assumed to be a function of only the energy in the ‘‘hopping’’ coordinate. Rewriting the Heaviside function as the integral of δ function we can write Eq. (19) as:

$$\begin{aligned}
 N(E) &= 2(2\pi\hbar)^{-(F-1)} \int_0^{E-E_c} dE_s \chi_r(E_s) \int d\mathbf{p}_Q \int d\mathbf{Q} \\
 &\quad \times \delta[E - E_c - E_s - H^{F-1}(\mathbf{p}_Q, \mathbf{Q})] \\
 &\equiv 2 \int_0^{E-E_c} dE_v P_{\text{tr}}(E - E_c - E_v) \rho_{F-1}(E_v), \quad (20)
 \end{aligned}$$

where E_c is the energy of the MSX, and E_v denotes energy in the “bound” modes on the seam. The physical meaning is very clear; the cumulative reaction probability is nothing but a weighted sum of density of states at the MSX.

From Eq. (20), it is easy to derive the quantum mechanical correspondence by rewriting the integral as the discrete sum over quantized vibrational states,

$$N(E) = 2 \sum_{\{n\}} P_{\text{tr}}[E - E_{v\{n\}}]. \quad (21)$$

It is seen that the simplest TST expression Eq. (21) for nonadiabatic process is very similar to the tunneling corrected TST expression (7). The Wigner tunneling transmission coefficient is replaced here by a diabatic transition probability. However, there is a fundamental difference between the two formulas. One can, in principle, carry out normal mode analysis all along the reaction path. Therefore, an *adiabatic* theory exists for Eq. (7), where instead of simply using an energy shift at the saddle point in the Wigner transmission coefficient, one can solve for the one-dimensional (1D) transmission coefficient rigorously with the potential corresponding to each adiabatic level. For the nonadiabatic transition problem, as mentioned earlier, we can carry out the normal mode analysis on the seam of crossing in a well-defined manner only at the MSX. Therefore, a simple adiabatic theory does not exist within the current framework.

C. General practical considerations

The practical evaluation of Eq. (21) can be accomplished with the direct counting procedure¹³ where one simply initializes the counting array to be the transition probability as a function of the energy in the “hopping” coordinate. As to the calculation of the transition probability factor $P_{\text{tr}}(E)$, in principle any formula can be used including the well-known Landau–Zener,²³ those of Nakamura and Zhu,²⁴ and distorted wave results for linear potentials from Child *et al.*,²⁵ as far as they are well-behaved in most of the energy range for the particular case one is interested in. Alternatively, one may construct a 1D model out of the realistic transition process, calculate the 1D transition probability as rigorously as possible, and substitute back into Eq. (21). In sec. III, we shall discuss how this has been done in the case of $\text{CH} + \text{N}_2$.

One may envisage a number of extensions of expression (21). First of all, in some cases, the assumption of uniform transition probability on the seam may not be adequate. A practical way to take the $\{\mathbf{Q}\}$ dependence of the transition probability (characteristic function) into account is to employ a “vibrationally adiabatic” approach. One calculates the expectation value of the coupling potential for each vibrational state and uses it as an effective coupling element in the 1D transition probability formula. It should be noted that one

does not have to do so for all the $\{\mathbf{Q}\}$ degrees of freedom, but only for a few that strongly influence the coupling element.

Furthermore, one seeks the possibility of extending (21) to nonadiabatic processes belonging to case IIA or IIB. As mentioned in the beginning of Sec. II B, there are two main difficulties for cases IIA and IIB. First, in contrast to case I, the coupling elements cannot be clearly defined in a general sense if one chooses to work in the diabatic representation. Approximate diabatization schemes have to be employed to abstract the coupling elements, a subject itself occupying extensive literature and shall not be discussed further here.²⁶ Second, both cases IIA and IIB require at least two degrees of freedom to describe the transition processes and therefore to derive the transition probability. In case IIA, for instance, although the degenerate condition is only onefold, the two electronic states do not interact unless the symmetry is lowered. Therefore, at least two degrees of freedom are essential, one symmetry-conserving mode describing the degeneracy condition (such as \hat{s} in the previous discussions) and one symmetry-breaking mode describing the nuclear motion that actually promotes the transition. Assuming that both issues can be solved, it is not hard to find the expression of the rate constant for the reaction using the similar approach listed in Sec. II B, except that the normal mode analysis has to be carried out in $3N-8$ dimensional space. Interestingly, one can compare the situation to that between the rate theories based on reaction path and reaction plane. Such extensions will be pursued in the near future.

To summarize Sec. II briefly, we have demonstrated that one can make a straightforward extension of the transition state theory to deal with nonadiabatic processes. In the current formulation, the seam surface is taken to be the dividing surface where the reaction flux is evaluated. Rather than picking an arbitrary representation of the seam,^{7(a)} or generating the seam numerically,^{7(b)} we have employed a Taylor expansion around the MSX to represent the seam. With the further assumption that the transmission coefficient is uniform on the seam, we have shown that the CRP can be written simply as Eq. (21), i.e., a weighted sum of density of states at the MSX by the 1D nonadiabatic transmission probability. Compared to earlier versions of nonadiabatic TSTs, the current formulation is more general in terms of the definition of the seam surface, the reaction coordinate (or the “hopping” coordinate), and the bound vibrational frequencies at the MSX. Therefore, we expect that the current formulation should be applicable to general polyatomic systems. In Sec. III, we apply the theory to an interesting and challenging spin-forbidden system: $\text{CH}(^2\Pi) + \text{N}_2 \rightarrow \text{HCN} + \text{N}(^4S)$.

III. APPLICATION OF THE NONADIABATIC TST THEORY TO $\text{CH}(^2\Pi) + \text{N}_2 \rightarrow \text{HCN} + \text{N}(^4S)$

The reaction of $\text{CH}(X^2\Pi) + \text{N}_2 \rightarrow \text{HCN} + \text{N}(^4S)$ is of great importance in combustion chemistry, and has been the subject of numerous experimental^{27,28} as well as theoretical studies.^{8,29–33} As to the mechanism of the reaction, it is well accepted that the dominant channel involves an intersystem crossing between the doublet and the quartet electronic states around a C_{2v} configuration, as schematically shown in Fig.

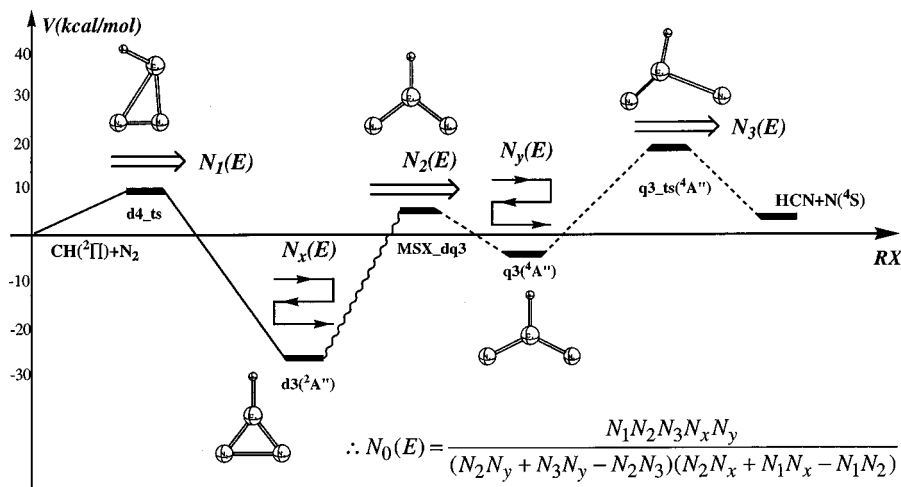


FIG. 1. Simplified schematic PES for the $\text{CH}(^2\Pi) + \text{N}_2 \rightarrow \text{HCN} + \text{N}(^4S)$ reaction used in the dynamical study of Seideman *et al.* and in the rate constant calculations in the current study.

1. Other channels have been discovered, but they are too high in energy to be important in most thermal conditions.⁸ A strong motivation for theoretical prediction of the rate constant is that reliable experimental data are not available for the most important temperatures, as emphasized by Miller and Walch.^{33(b)} Furthermore, the relatively complicated feature of the potential surface of this system makes it challenging and interesting to investigate the underlying dynamics of the process.

Most relevant to the current study, a set of two-dimensional (2D) model potential surface for the channel involving C_{2v} doublet minima has been constructed by Seideman and Walch.³² In this study, the reaction was viewed as two unimolecular decay processes coupled via spin-orbit interaction. The cumulative reactive probability was then calculated with the Fermi golden rule using the resonance wave function of the doublet and quartet states, and the spin-orbit coupling element from the earlier work of Yarkony *et al.*²⁹ The J -shifting approximation along with the centrifugal sudden approximation was used to calculate the thermal rate constants. Overall, the reaction probability was found to exhibit a resonance structure which changes from a series of sharp isolated line shapes at low energies to broader overlapping ones at higher energy. The extrapolated thermal rate constant agreed reasonably well with experimental measurements. In another recent work,^{33(a)} empirical RRKM theory has been used to obtain the rate constant and its pressure dependence. However, several key parameters such as the intersystem crossing transmission coefficient and the vibrational frequencies of the MSX were adjusted to fit experimental measurements rather than derived from the first principled study. Finally, in a recent study of Walch and Miller,^{33(b)} the rate constant was calculated assuming that the intersystem crossing process is fast compared to the barrier crossing processes on the doublet and the quartet states. Consequently, the rate constant is related to the transition states on the doublet and quartet states only. Although their results agree rather well with experimental measurements, our results do not support their essential assumption of fast surface hopping motion. We will apply our newly derived nonadiabatic TST to the titled reaction, and compare the results to those from these recent studies.

A. Construction of model and formula for the rate constant

In the current study, we have employed the reduced dimensionally picture as in the 2D quantum mechanical study of Seideman *et al.*,³² which is illustrated in Fig. 1. The dative channel⁸ will not be included in the current study, although it will be interesting in the future to include this channel via the V-RRKM theory to obtain the rate constant for the $\text{CH}(^2\Pi)$ disappearance. As illustrated in Fig. 1, the entire process of the $\text{CH}(^2\Pi) + \text{N}_2 \rightarrow \text{HCN}$ reaction has been divided into three stages: (i) overcoming the barrier $\mathbf{d4_ts}$ to form $\mathbf{d3}$, (ii) intersystem crossing from the doublet $\mathbf{d3}$ to the quartet state $\mathbf{q3}$ through the region around $\mathbf{MSX_dq3}$, and (iii) overcoming the barrier $\mathbf{q3_ts}$ to form the quartet product $\text{HCN} + \text{N}(^4S)$. Within the spirit of TST, we treat each step *independently* and finally combine them to obtain the rate constant for the entire process. There are a few different ways to combine the components, and we have chosen to follow the spirit of the unified statistical theory (UST) of Miller,³⁴ noting that we have two rather deep complexes $\mathbf{d3}$ and $\mathbf{q3}$.

The UST has been designed to unify TST, which is suited for direct dynamics across a barrier, and the phase space theory (PST), which is suited for reactions with a long-lived complex in a deep well. In the original derivation, a reaction profile with one entrance TS, one complex, and one exit TS is assumed. Briefly, the total CRP $N_0(E)$ can be written as:

$$N_0(E) = P_{b \leftarrow a}(E) N_a(E), \quad (22)$$

where $P_{b \leftarrow a}(E)$ defines the portion of the flux going from the reactant a to product b . The expression for $P_{b \leftarrow a}(E)$ in terms of the $N(E)$ at each critical structure has been analyzed by Miller using the branching picture of Wigner (1932), and the derived formula after a geometrical series sum is given by

$$P_{b \leftarrow a} = \frac{P_{b \leftarrow x} P_{x \leftarrow a}}{1 - (1 - P_{b \leftarrow x})(1 - P_{a \leftarrow x})}, \quad (23)$$

where $P_{x \leftarrow a} = N_1/N_a$ and $P_{b(a) \leftarrow x} = N_{2(1)}/N_x$. Here a and b

TABLE I. Parameters used in the nonadiabatic TST calculation for the reaction of CH+N₂.

| Structure | Frequencies ^a (cm ⁻¹) | Energy ^b (kcal/mol) | Rotational const. (GHz) | μ_{1D} ^c |
|--|---|--------------------------------|---|-------------------------|
| CH(² Π),N ₂ | 2804.3, 2447.0 <i>2831.1, 2340.5</i> | 0.0 <i>0.0</i> | 426.8(×2);60.1(×2) <i>426.4(×2);58.7(×2)</i> | |
| d4_ts (² A) | 300.9, 600.4, 1036.2, 1900.7, 3008.2 <i>271.3, 654.2, 973.0, 1763.3, 3073.9</i> | 8.5 <i>11.8</i> | 52.2, 19.9, 14.6 <i>51.4, 20.5, 14.8</i> | |
| d3 (² A ₂) | 718.1, 838.7, 926.3, 1193.3, 1636.4, 3206.2 <i>650.5, 857.6, 925.6, 1212.0, 1610.2, 3256.0</i> | -28.2 <i>-25.6</i> | 41.4, 29.1, 17.1 <i>41.2, 28.1, 16.7</i> | |
| MSX_dq3 (³ A ₂) | 943.2, 948.3, 1370.7, 1476.0, 3025.8 | ... | 63.5, 16.6, 13.2 | 16 242.8 |
| MSX_dq3 (⁴ B ₁) | 797.4, 1005.0, 1059.7, 1358.6, 3040.8 <i>785.2, 965.8, 1101.1, 1298.9, 3079.8</i> | 0.4 <i>-0.1</i> | 63.5, 16.6, 13.2 <i>68.2, 15.2, 12.4</i> | |
| q3 (⁴ B ₁) | 562.0, 809.1, 1103.4, 1187.4, 1225.2, 2886.5 <i>551.2, 804.5, 1038.1, 1190.6, 1216.9, 2986.1</i> | -1.9 <i>-5.6</i> | 98.0, 13.1, 11.5 <i>94.5, 13.0, 11.4</i> | |
| q3_ts (⁴ A'') | 349.2, 741.1, 866.2, 1929.5, 3294.6 <i>375.2, 718.7, 910.3, 1823.9, 3267.3</i> | 19.5 <i>15.5</i> | 68.2, 10.0, 8.7 <i>70.4, 10.4, 9.1</i> | |

^aNumbers are derived from the B3LYP/6-311G(*d,p*) calculations of Ref. 8, and italic numbers are derived from the UCCSD(T)/6-311G(*d,p*) calculations.

^bNumbers are G2M-RCC results from Ref. 8, which do not include the zero-point energies (ZPE), and italic numbers are UCCSD(T)/PVTZ results without ZPE. For **MSX_dq3**, only the averaged energy of the doublet and quartet states is given.

^cReduced mass in the 1D effective Hamiltonian, in units of a.u.

denote reactants and products, respectively, and 1(2) and *x* denote the entrance (exit) barrier and the complex, respectively. It can be shown that Eq. (23) goes to both the PST and TST limit correctly.

Within the same spirit, we have extended Eq. (23) to our

system where there are two deep complexes and three transition states, among which **MSX_dq3** has been viewed as a standard transition state as discussed previously. Straightforward derivation (see the Appendix for details) leads to the following expression for $P_{b\leftarrow a}(E)$ ³⁵

$$P_{b\leftarrow a}(E) = \frac{P_{b\leftarrow y}P_{y\leftarrow x}P_{x\leftarrow a}}{[1 - (1 - P_{x\leftarrow y})(1 - P_{b\leftarrow y})][1 - (1 - P_{y\leftarrow x})(1 - P_{a\leftarrow x})]}, \quad (24)$$

where $P_{x\leftarrow a} = N_1/N_a$, $P_{a\leftarrow x} = N_1/N_x$, $P_{y\leftarrow x} = N_2/N_x$, $P_{x\leftarrow y} = N_2/N_y$ and $P_{b\leftarrow y} = N_3/N_y$. Here, 1, 2, and 3 denote the first, second (**MSX**) and third transition state, respectively, and *x* and *y* denote the first and second complex, respectively, as shown in Fig. 1.

Substituting Eq. (24) into Eq. (22), we get the following expression for $P_{b\leftarrow a}(E)$ in terms of the $N(E)$ at each critical structure:

$$P_{b\leftarrow a}(E) = \frac{N_1 N_2 N_3 N_x N_y}{N_a (N_2 N_y + N_3 N_y - N_2 N_3) (N_2 N_x + N_1 N_x - N_2 N_1)}. \quad (25a)$$

It is interesting to note that in the limit where the intersystem crossing is rate determinant, namely $N_2 \ll N_x, N_y$, we have $P_{x(y)\leftarrow y(x)} \ll 1$, and Eq. (25a) reduces to:

$$P_{b\leftarrow a}(E) = \frac{P_{y\leftarrow x}P_{x\leftarrow a}}{P_{a\leftarrow x}} = \frac{N_2}{N_a}. \quad (25b)$$

In other words, the CRP for the entire reaction will reduce to $N_2(E)$, which is intuitively correct.

In the calculation of all the individual $N(E)$'s in Eq. (25), we have used harmonic direct counting at each critical

structure. The energetics and vibrational frequencies used in the rate calculation are summarized in Table I. We have not included the tunneling correction at the transition state 1 or 3, since the effect is expected to be small. To calculate the $N_2(E)$ at **MSX_dq3**, we have used the projected vibrational frequencies calculated in our previous work⁸ with the algorithm listed in Sec. II. Another ingredient in the calculation of $N_2(E)$, the transition probability as a function of energy in the hopping coordinate \hat{s} , will be discussed later.

To obtain the thermal rate constant, we need to carry out the Boltzmann average of the microcanonical rate constant as the following:

$$k(T) = [2\pi\hbar Q_r(T)]^{-1} \int_{-\infty}^{\infty} dE e^{-\beta E} \sum_{J=0}^{\infty} (2J+1) \times \sum_{K=-J}^J N_0^{JK}(E), \quad (26)$$

where the $N_0^{JK}(E)$ is obtained by using the shifted energy $E - E_{JK}^R$ in Eq. (25), and different rotational constants (*B*, *C*) at different structures have been used to carry out the symmetric top rotational energy shifting within the spirit of the

adiabatic rotation theory of Bowman *et al.*³⁶ If one assumes that rotational constants do not change significantly among the critical structures, one may use one set of rotational constants, and Eq. (26) can be further simplified in a straightforward manner as shown previously,³⁷

$$k(T) = \frac{Q_{\text{rot}}^{\ddagger}}{h Q_{\text{tr}} Q_{\text{rot}} Q_{\text{vib}}} \int_0^{\infty} dE e^{-\beta E} N_0^{00}(E). \quad (27)$$

B. The 1D nonadiabatic transition probability

As discussed above, virtually any formula can be used for the 1D nonadiabatic transition probability in the calculation of CRP at the MSX, as far as it is well-behaved for the particular system. The most desirable choice is to solve for the 1D transition probability quantum mechanically, which is the approach adapted in the current study. For the current system, it is clear from the structure of **d3**, **q3**, and **MSX_dq3** that the ‘‘hopping’’ coordinate is nearly exclusively in the N–C–N bending. Treating CH as a united atom, the 1D bending Hamiltonian is straightforwardly written down as the following as in a triatomic with fixed bond distances:³⁸

$$H = \frac{1}{2} \left(-i\hbar \frac{\partial}{\partial \theta} \right) G_{\theta\theta} \left(-i\hbar \frac{\partial}{\partial \theta} \right) + V(\theta; R) + V'(\theta; R),$$

$$G_{\theta\theta} = \frac{2}{\mu_{\text{CH,N}} R^2} - \frac{2 \cos \theta}{m_{\text{N}} R^2}, \quad (28)$$

$$V'(\theta; R) = \frac{\hbar^2}{2m_{\text{B}} R^2} \cos \theta - \frac{\hbar^2}{8} G_{\theta\theta} (1 + \csc^2 \theta),$$

where the last term is usually assumed to be small in most cases despite the singularity at $\theta = \pi$.³⁹ Neglecting the V' term and expanding the kinetic term, one obtains the following 1D bending differential equation:

$$\left[-\hbar^2 \left(\frac{2}{\mu_{\text{CH,N}} R^2} - \frac{2 \cos \theta}{m_{\text{N}} R^2} \right) \frac{\partial^2}{\partial \theta^2} - \hbar^2 \frac{2 \sin \theta}{m_{\text{N}} R^2} \frac{\partial}{\partial \theta} + V(\theta) - E \right] \times \Psi(\theta) = 0. \quad (29)$$

The first derivative term can be eliminated with a standard technique, and Eq. (29) becomes simplified as:

$$A \Phi'' - \left(V - \frac{B^2}{4A} - E \right) \Phi = 0, \quad (30)$$

$$A = -\hbar^2 \left(\frac{2}{\mu_{\text{CH,N}} R^2} - \frac{2 \cos \theta}{m_{\text{N}} R^2} \right), \quad B = -\hbar^2 \frac{2 \sin \theta}{m_{\text{N}} R^2}.$$

The term

$$\frac{B^2}{4A} = \frac{\hbar^2}{2R^2} \left(\frac{\mu_{\text{CH,N}} \sin^2 \theta}{m_{\text{N}}^2 - m_{\text{N}} \mu_{\text{CH,N}} \cos \theta} \right)$$

is only on the order of 1.0×10^{-6} hartree with the parameters of the **MSX_dq3**, and therefore can be safely neglected.

In order to carry out calculation of the transition probability with the Hamiltonian defined in Eq. (30), we need the

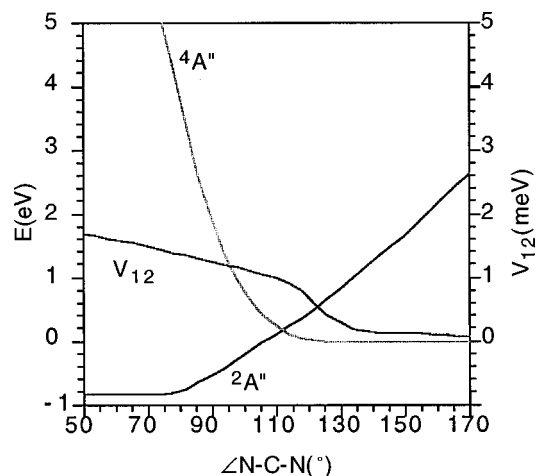


FIG. 2. The 1D model potential energy curves (${}^2A''$ and ${}^4A''$) as functions of N–C–N angle θ , constructed to obtain the diabatic transition probability between them. The energies are in electron volts, with that of ${}^4A''$ state set to 0. The spin–orbit coupling constants V_{12} are shown in millielectron volts.

1D potential energy curves and spin–orbit coupling elements. We have carried out CASPT2/6-311G(d,p)⁴⁰ calculations with the (nine electron/nine orbital)-complete active space self-consistent field (CASSCF) references along the N–C–N bending coordinate from **d3** to **q3**, with other parameters fixed at those of **MSX_dq3** optimized at the UCCSD(T)/6-311G(d,p) level. The CASPT2 method is chosen in the curve scan to be consistent with the CASSCF method which has been used to calculate the spin–orbit coupling elements.⁸ The potential energy curves have then been shifted to match with the more reliable energy calculated at the G2M(RCC)⁴¹ level with the zero-point correction.⁸ Furthermore, we artificially flattened out the potential energy curves of the doublet (quartet) when the N–C–N angle is smaller (larger) than that in the **d3**(**q3**) to model the asymptotes for scattering calculation. We also artificially made the doublet potential energy go up more quickly with the N–C–N angle near the **q3** structure to make sure that only the quartet asymptote is accessible at **q3**. It should be noted that we expect the spin-forbidden process to be rather localized around the crossing point in this 1D model, judging from the relatively large gradients of the potential energy curves around the crossing point. Therefore, we expect that these artificial modifications of the potential curves in the regions far from the crossing point will not alter the transition probability seriously. Furthermore, despite these changes, the present potential curves and coupling elements are far more realistic than the linear potential/constant coupling model assumed in many transition formulas.

The resultant 1D potential energy curves and the spin–orbit coupling element are shown in Fig. 2. Note that the spin–orbit coupling elements $V_{12} = \langle \frac{1}{2}, \pm \frac{1}{2} | H^{SO} | \frac{3}{2}, \pm \frac{3}{2} \rangle$ are shown in meV. As seen in Fig. 2, the energy separation increases dramatically as the N–C–N angle deviates from 111.2° in **MSX_dq3**, which implies that the transition is very localized. Therefore, the angle θ in the kinetic energy operator of Eq. (30) is treated as a constant taken from the value at

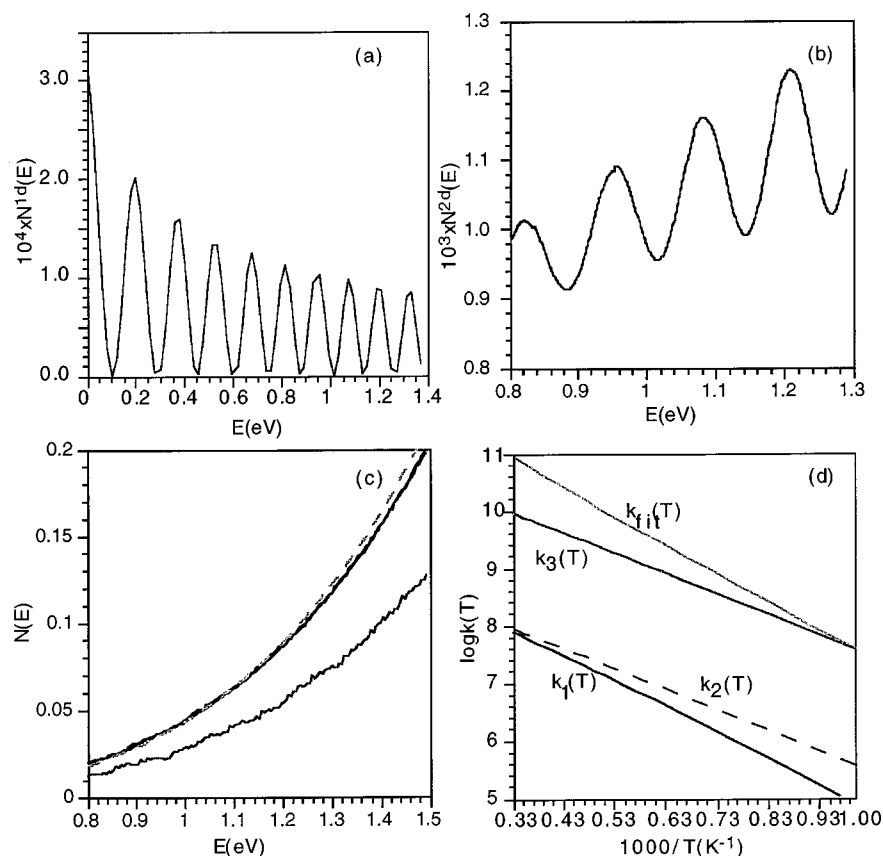


FIG. 3. (a) 1D transition probability obtained with the distorted wave approximation as a function of energy (electron volts). In (a), the energy of $\mathbf{q3}$ is set to 0, while in (b) and (c) energies are relative to the zero-point level of the reactants. (b) 2D cumulative reaction probability $N_2^{2D}(E)$ obtained by energy shifting approximation based on $N_2^{1D}(E)$ as a function of energy (electron volts). The frequency for the bound degree of freedom is selected to be the asymmetric C–N stretch of the $^2A''$ state at **MSX_dq3**. (c) $N_0(E)$ for the total reaction calculated according to Eq. (25). The solid curves are obtained with G2M-RCC energetics and B3LYP/6-311G(*d,p*) vibrational frequencies; the relatively smooth solid curve is obtained with the vibrational frequencies of the $^4A''$ state at **MSX_dq3**, and the solid curve with more visible structures is calculated with those of the $^2A''$ state at **MSX_dq3**. The dashed curve is calculated with the UCCSD(T)/PVTZ energetics and UCCSD(T)/6-311G(*d,p*) vibrational frequencies, and for **MSX_dq3** the frequencies of the $^4A''$ state are used. The total $N_0(E)$ is actually very close to $N_2(E)$ calculated at **MSX_dq3**, which if included in Fig. 3(c) would not be distinguished graphically. (d). Thermal rate constants for the production of quartet products calculated according to Eq. (27). The $k_1(T)$ is obtained with the G2M-RCC energetics and B3LYP/6-311G(*d,p*) vibrational frequencies, $k_2(T)$ is obtained with the UCCSD(T)/PVTZ energetics and UCCSD(T)/6-311G(*d,p*) vibrational frequencies. $k_3(T)$ is computed with scaled vibrational frequencies of **MSX_dq3** taken from Ref. 33 and two times larger spin–orbit coupling constant. $k_{fi}(T)$ is from Ref. 33.

MSX_dq3 through the scattering calculations.

Once the 1D model is established, we first tried to solve for the transition probability $N_2^{1D}(E)$ by the flux–flux correlation function method of Miller *et al.*⁴ in conjunction with the complex L^2 method, which has been successfully applied to a model 1D non-adiabatic reaction by Qi and Bowman.⁶ Unfortunately, it was found that the cumulative reaction probabilities exhibit a wild oscillatory behavior as the basis set size and the absorbing potential are changed. Evidently, with a spin–orbit coupling element of only ~ 10 cm^{-1} , the transition probability in the current case is so small that it is beyond the numerical accuracy expected from the complex L^2 methods. Therefore, we have finally carried out scattering calculations with the distorted wave approximation (DWA),²⁵ which is expected to be rather reliable for the current system with such small diabatic coupling elements.⁴² The transition amplitude, the square root of the transition probability, from DWA is simply given by

$$T_{fi} \equiv \sqrt{N_2^{1D}} = 2(k_f k_i)^{-1/2} \int_0^\infty \psi_i^{(0)}(r') V_{if}(r') \psi_f^{(0)}(r') dr', \quad (31)$$

where $V_{if}(r)$ is the diabatic coupling element, and $\psi_i^{(0)}(r)$ and $\psi_f^{(0)}(r)$ are the scattering wave functions associated with each diabatic potential.

The transition probability $N_2^{1D}(E)$ thus calculated as a function of energy is presented in Fig. 3(a). Evidently, the DWA exhibits oscillations in the transition probabilities, a phenomena first pointed out by Stückleberg, which manifests the interference between the trajectories on the two diabatic surfaces. The absolute values for the transition probabilities are very small, on the order of 10^{-4} . Evidently, the reaction is very “diabatic” even around the MSX regions. The 1D transition probabilities using the semiclassical results of Child *et al.*²⁵ assuming linear crossing potentials have also been calculated as a function of the energy in the hopping

coordinate (not included here). The results are slightly smaller in magnitude and exhibit milder oscillations as a function of energy.

C. Convolved rate constant $N(E)$ and $k(T)$

Before presenting results for convoluted $N(E)$ and $k(T)$, we briefly discuss the degeneracy factors in the CRP expression coming from spatial and spin symmetries. The reactant $\text{CH}^2(\Pi)$ has double degeneracy for the Π spatial symmetry. Nevertheless, only the $^2A''$ state is expected to lead to the titled reaction, therefore no degeneracy needs to be considered for the reactant partition function, except for the electronic part taken as $[1 + \exp(-25.8/T)]$ following Ref 33(b). In addition, since the reaction proceeds through a spin-forbidden transition from the doublet to the quartet state, it appears that a factor of 2 should be considered in the transition probability, due to the increase of spin-multiplicity, i.e., the number of microstates. However, the situation is more complicated as the following. According to the well-known Eckart–Wigner theorem, the nonvanishing spin–orbit coupling elements between 2A_2 and 4B_1 are:

$$\langle \frac{1}{2}, \pm \frac{1}{2} | H^{so} | \frac{3}{2}, \pm \frac{3}{2} \rangle = \sqrt{3} \times \langle \frac{1}{2}, \pm \frac{1}{2} | H^{so} | \frac{3}{2}, \mp \frac{1}{2} \rangle. \quad (32)$$

Therefore according to Eq. (31), the probability of the molecule making transition from $|\frac{1}{2}, \pm \frac{1}{2}\rangle$ to $|\frac{3}{2}, \pm \frac{3}{2}\rangle$ is 3 times larger than that to $|\frac{3}{2}, \mp \frac{1}{2}\rangle$, and the transitions to $|\frac{3}{2}, \pm \frac{1}{2}\rangle$ and $|\frac{3}{2}, \mp \frac{3}{2}\rangle$ are forbidden. As a result, one may multiply a factor of $\frac{4}{3}$ by the transition probability calculated between $|\frac{1}{2}, \pm \frac{1}{2}\rangle$ and $|\frac{3}{2}, \pm \frac{3}{2}\rangle$. However, we did not do so in the current work to be consistent with previous 2D quantum mechanical calculations of Seideman *et al.*^{32(b)}

To compare the current work to the 2D study of Seideman,^{32(b)} we convoluted the $N_2^{1D}(E)$ with one vibrational frequency to model the effect of an extra degree of freedom. Since this degree of freedom in Seideman's work is mostly the C–N stretch, we have taken the frequency of 943 cm^{-1} (which is 1005 cm^{-1} for the quartet state) corresponding to the asymmetric C–N stretch mode at **MSX_dq3**. The derived results, denoted as $N_2^{2D}(E)$, are plotted in Fig. 3(b). The $N_2^{2D}(E)$ is on the order of 10^{-3} , and exhibits some moderate oscillations, much less sharper than those from Seideman's 2D $N(E)$ [Figs. 3–5 in Ref. 32(b)]. Since the 2D $N(E)$ from Ref. 32(b) is available only for very limited energy range and is highly oscillatory, it is hard to compare it quantitatively with our $N_2^{2D}(E)$. The qualitative trend is that our $N_2^{2D}(E)$ is larger in the low energy but becomes smaller in magnitude than Seideman's as energy increases. For instance, the $N_2^{2D}(E)$ is ~ 1.0 and 1.15×10^{-3} at $E=0.8$ and 1.1 eV in Fig. 3(b). In the calculations from Ref. 32(b), the peak value of $N(E)$ around $E=0.8$ and 1.1 eV is 1.5×10^{-4} [Fig. 3 in Ref. 32(b)] and 1.6×10^{-2} [Fig. 4(a) in Ref. 32(b)], respectively.

Next, we have calculated $N_0(E)$ for the entire reaction according to Eq. (25). The $N_0(E)$ result for $J=0$ has been presented in Fig. 3(c). A number of calculations have been done using different energetic and frequency parameters to test the sensitivity of the results on the level of *ab initio* calculations. First of all, two sets of vibrational frequencies, obtained at the $^2A''$ and $^4A''$ electronic states at **MSX_dq3**

have been tested. The energetics at the G2M-RCC level and vibrational frequencies at the B3LYP/6-311G(*d,p*) level shown in Table I have been used, and the resultant $N_0(E)$ are shown in solid curves in Fig. 3(c). Clearly, the $N_0(E)$ shows interesting structures even after the convolution of the five vibrational degrees of freedom which are more visible when the frequencies for the $^2A''$ state at **MSX_dq3** are employed in the calculations. In addition, the $N_0(E)$ obtained with frequencies for the $^4A''$ state at **MSX_dq3** are larger than that calculated with those for $^2A''$, since the numerical values of the frequencies are generally smaller for the former. During the calculation, we notice that the total $N_0(E)$ is actually very close to the $N_2(E)$ calculated at **MSX_dq3**, which if included in Fig. 3(c) cannot be distinguished graphically. The transition probability at **MSX_dq3** is so small, as discussed earlier, that the total $N_0(E)$ reduces to the $N_2(E)$ at **MSX_dq3**, as indicated in Eq. (25). In a second set of calculations of $N_0(E)$, we have used the energetics derived at the UCCSD(T)/PVTZ level, and the vibrational frequencies at the UCCSD(T)/6-311G(*d,p*) level. For **MSX_dq3**, the vibrational frequencies for the $^4A''$ state are used. The resultant $N_0(E)$, shown as a dashed line in Fig. 3(c) is in close agreement with the result discussed above. This is not surprising since the $N_0(E)$ is mainly determined by the properties (energetics and vibrational frequencies) of the MSX, which, as shown in Table I, have similar values for the different levels of theories used in the current calculations.

Since **MSX_dq3** is the rate determining structure, we have simply employed J shifting to derive the thermal rate constant according to Eq. (27), with the rotational partition function of **MSX_dq3**. The $N_0(E)$ used in the calculation of $k(T)$ is averaged with values obtained with the vibrational frequencies of the doublet and quartet states. In the integration over energy in Eq. (27), the $N_0(E)$ has been extrapolated with a power law (~ 5 , with a correlation coefficient of 0.999) to high energies (up to 3.0 eV above the reactants) to ensure the convergence of the calculated thermal rate constant. Preliminary test calculations indicate that the discrepancy between $k(T)$ from Eqs. (26) and (27) should be small, around 60% at 1000 K. In essence the physical picture of the reaction behind the approximation here is the following. The threshold of the reaction [i.e., the integration threshold in Eq. (27)] is controlled by **q3_ts**, due to its high energy. As soon as the quartet channel is open, however, the reaction flux bottleneck is shifted to the doublet-quartet crossing, since the hopping probability is so small. As in the calculation of $N_0(E)$, two sets of data have been used to calculate $k(T)$ to see the sensitivity of the result on the levels of *ab initio* theories employed in deriving the necessary information. The resultant $k(T)$ at the temperature range of 1000–3000 K is shown in Fig. 3(d). The $k_1(T)$ is calculated with the G2M-RCC energetics and the B3LYP/6-311G(*d,p*) vibrational frequencies, and $k_2(T)$ is calculated with the UCCSD(T)/PVTZ energetics along with the UCCSD(T)/6-311G(*d,p*) vibrational frequencies. The numerical values of the two sets of data are in close agreement except that the UCCSD(T)/PVTZ method gives a lower exit barrier on the quartet surface than G2M-RCC, which results in a larger rate constant

at low temperature ~ 1000 K. At high temperature around 3000 K, however, the rate constants predicted with the two sets of data tend to agree. The calculated $k(T)$ can be accurately fitted into an Arrhenius expression with a prefactor of $10^{9.39}$ and $10^{9.17}$ for k_1 and k_2 , respectively, which seems to be too low compared to the recent experimental measurements and empirical RRKM studies, which has a prefactor $\sim 10^{11-12}$. Given the high level of our *ab initio* calculations and the reasonable agreement of k_1 and k_2 , the rather large discrepancy cannot be attributed to the error from the *ab initio* calculations.

In the previous empirical RRKM results of Rogers *et al.*,^{33(a)} shown as $k_{\text{fit}}(T)$ in Fig. 3(d), they mentioned that a much smaller rate constant is obtained compared to experimental measurement unless several empirical frequencies at the MSX are scaled down by a factor of 2 and at the same time a very large κ value of 0.04 (even larger than the Landau–Zener probability of 0.001–0.01 by Yarkony *et al.*²⁹) is used to describe the intersystem crossing probability. Indeed, the scaled results contain three frequencies around 300 cm^{-1} , which are substantially lower than what we have obtained in *ab initio* calculations in Table I. With their vibrational frequencies, we found that our rate constant increased by more than an order of magnitude. Further assuming that the spin–orbit coupling element is two times larger than what we have calculated, we have obtained a thermal rate constant $k_3(T)$ in Fig. 3(d), which is in closer agreement to $k_{\text{fit}}(T)$. Evidently and very importantly, scaling the frequencies and the coupling element is not a real solution to the problem. The disagreement between the *ab initio* thermal rate constant $k_3(T)$ and the fitted $k_{\text{fit}}(T)$ rather strongly suggests that some important issues might have been overlooked which required further investigations as we will suggest later.

In another RRKM study of Miller and Walch,^{33(b)} the rate constant was calculated assuming that the surface hopping process is fast compared to the barrier crossing motion and therefore the rate constant is solely determined by the two transition states:

$$k(T) = [hQ_R(T)g_e(T)]^{-1} \sum_J (2J+1) \times \int \frac{g_1 N_1(E, J) g_2 N_2(E, J)}{g_1 N_1(E, J) + g_2 N_2(E, J)} e^{-E/k_B T} dE, \quad (33)$$

where $N_1(E)$ and $N_2(E)$ are measured at **d4_ts** and **q3_ts**, respectively. The energetics and rotational/vibrational parameters were derived in the earlier study of Walch,³¹ which is in fair agreement with our results. It should be noted that the barrier heights in their studies^{33(b)} are *higher* than ours by ~ 4 kcal/mol for both **d4_ts** and **q3_ts**. Interestingly, their calculations agree well with the experimental measurements. We have also carried out some test calculations following Eq. (33) but with our *ab initio* data. It turned out that the obtained $k(T)$ is rather similar in magnitude to the results in Ref. 33(b), which therefore rules out the possibility of some simple numerical error in our calculations. Comparing the CRP corresponding to Eq. (33) and in Eq. (27), it is not surprising that the former is much larger in magnitude by an

order of 2–4, which after integration naturally yields a larger thermal rate constant that is ironically closer to the experimental value. Clearly, the physical pictures in the current study and that of Miller and Walch^{33(b)} are of two extremes. In our approach, as mentioned earlier, the **MSX_dq3** is the rate determining step due to the small intersystem crossing probability, while **q3_ts** controls the threshold of the reaction. In the formulation of Miller *et al.*,^{33(b)} the contrary picture is adopted in which the surface hopping is not related to the rate constant at all, and two standard chemical barriers form the “standard” RRKM scenario. Although the $k(T)$ from Ref. 33(b) is closer (much closer!) to experimental measurements than our results, it is hard for us to accept the picture that a hopping process with very small transition probability is not relevant to the rate of the process. It appears to us that the good agreement between Ref. 33(b) and experiments may be fortuitous.

The question is then, what could be responsible for the discrepancy between our results and experimental measurements? As mentioned earlier, given the high level of our quantum chemical calculations and the fact that the rate constants obtained with different sets of data agree reasonably well, it is very unlikely that the difference from the experimental data can be attributed to the *ab initio* methods used. Admittedly, there are several assumptions made in the 1D dynamics calculations, but the obtained spin-forbidden transition probability certainly looks reasonable given the small values of the spin–orbit coupling elements.

Thus, the large discrepancy between the theoretical value and the experimental data most likely comes from the current treatment of the multidimensional dynamics. For instance, although a one-dimensional model for the intersystem crossing appears very reasonable judging from the structure of **d3**, **MSX_dq3**, and **q3**, it is possible that another degree of freedom, which may or may not be the C–N stretch, is also very important for the spin-forbidden transition. By this we mean that the transition probability χ , which in the current work is assumed to depend only on the energy in the hopping coordinate, might actually vary significantly along one or more degrees of freedom orthogonal to the norm of the seam \hat{s} . We note that at the **q3** structure, the doublet electronic state is not very high in energy, and therefore the seam might cover a larger region of the PES at certain energy than that based on simple harmonic expansion at **MSX_dq3**. Indeed, as mentioned above the $N_2^{2D}(E)$ we obtained appears to increase too slowly as a function of energy, compared to the explicit 2D quantum mechanical result of Seideman.^{32(b)} It has also been found in previous studies that the 1D model may not be quantitatively satisfactory for nonadiabatic processes, since quantal transitions with small probabilities are likely to be sensitive to the coupling of the degree of freedom in which the nonadiabatic transition is nominally located and other rovibrational degrees of freedom.⁴³

In addition, we are concerned with the effect of gradient difference between the two PESs on the transition probability. In the Landau–Zener formalism, a larger gradient difference implies a smaller diabatic transition probability. At the **MSX**, the structure is rather far from the minima on either of

the PESs and therefore the slope difference is rather large (recall they have different signs) and the transition probability is small. For other structures on the seam that are closer to the quartet minima (as mentioned above, the doublet state is not much higher in energy than the quartet state at the **q3** structure), the slope difference might be smaller and the transition probability may be larger. In short, the topology of the seam may play an important role in determining the transition probability.

Therefore, rigorous quantum dynamic calculations with at least 2 degrees of freedom with accurate spin-orbit coupling elements in extended region and at the same time with approximate treatment of other degrees of freedom are required to examine the situation in more depth.

IV. CONCLUSIONS

The TST has been extended straightforwardly to treat nonadiabatic processes and has been applied to study the rate constant of the spin-forbidden reaction $\text{CH}(\text{II}) + \text{N}_2 \rightarrow \text{HCN} + \text{N}(\text{S})$. A one-dimensional model was set up to consider the spin-forbidden transition probability, which was solved with distorted wave approximation. The effect of other degrees of freedom is then considered by energy convolution with the vibrational frequencies orthogonal to the seam of crossing at the MSX. An expression of the total CRP of the reaction was obtained by a straightforward extension of the unified statistical theory (UST), where the MSX was treated as a transition state. The obtained $N(E)$ seems to be consistent with that obtained by Seideman^{32(b)} with the ABC-DVR-Fermi-golden-rule approach and a 2D model.

Nevertheless, with such a TST expression and the one-dimension model for the intersystem crossing process, the thermal rate constant $k(T)$ seems to be too low by two orders of magnitude compared to experimental measurements. For this system, we feel that the current one-dimension model needs further improvement to obtain an accurate $k(T)$. In particular, the assumption that the spin-forbidden transition takes place with uniform probability on the seam may be a poor assumption in the particular case we are considering. The transition probability is determined by the spin-orbital coupling element and the difference in the slope between the two potential surfaces at the seam. Considering that the electronic nature of the two potential surfaces is not changing much at the seam, it is not likely that the magnitude of the spin-orbit coupling element depends strongly on the location of the seam. The slope difference, on the other hand, can depend more sensitively on the seam geometry. It is of great importance to further investigate the origin of the discrepancy, so that we may achieve better understanding of the underlying dynamics of not only this particular reaction but systems involving intersystem crossing in general.⁴⁴

The vibrational frequencies obtained in the *ab initio* study are much larger than those used in an empirical RRKM study,^{33(a)} where empirical vibrational frequencies at the MSX have to be scaled by a factor of 2 along with a large surface hopping probability (0.04) in order to derive a reasonable $k(T)$. Such an empirical approach does not give any answer to the discrepancy found between the current calculation and experimental measurement, but rather the dis-

agreement strongly suggests that some important issues might have been overlooked. In another study of Miller and Walch,^{33(b)} it is assumed that the surface hopping process is fast compared to the barrier crossing motion and the resultant RRKM rate constants are rather close to the experimental measurements. However, it is hard for us to accept the physical picture that an intersystem crossing process with a small transition probability is not relevant to the rate constant. Therefore we feel that the agreement between their results and experimental measurement may be fortuitous.

Although our initial attempt to calculate a rate constant of the spin-forbidden reaction with a straightforward extension of TST did not produce numerically satisfactory results for the titled reaction, the approach discussed in the current work seems to be theoretically sound and practical for evaluation of the rate constant for polyatomic systems for the multistep reaction involving nonadiabatic transition. It is still of great interest to carry out calculations on other systems, such as $\text{N}_2 + \text{O}(\text{P})$, to test the validity of the TST approach developed here.⁴⁵ On the other hand, the current work also has demonstrated that nonadiabatic processes, even the simplest case of spin-forbidden transition, might involve more degrees of freedom than usually presumed, based on the critical structures involved.

ACKNOWLEDGMENTS

The authors thank Dr. T. Seideman for interesting discussions on the system, and sending data related to the figures in Ref. 32(b). Q.C. also thanks Professor M. C. Lin for discussions and encouragement and acknowledges a graduate fellowship from the Phillips Petroleum Co. S.J.K. acknowledges the Visiting Fellowship at the Emerson Center, which provided an opportunity for this collaboration. The use of computational facilities and software at the Emerson Center is acknowledged. This work was supported in part by Grant Nos. F49620-95-1-0182 and F49620-98-1-0063 to K.M. from the Air Force Office of Scientific Research. J.M.B. acknowledges financial support from the Department of Energy (DE-FG02-97 ER 14782).

APPENDIX DERIVATION OF THE REACTION PROBABILITY FOR A GENERAL DOUBLE-WELL PROBLEM WITH THE UST APPROACH

It should be noted that Eq. (24) is applicable for double-well cases with the following restriction: $N_x, N_y \gg N_1, N_3 \gg N_2$. In other words, the second transition state (i.e., the MSX in the current system) has to be the dominant bottleneck, which is the case for the titled reaction. For a general double-well problem, Eq. (24) has to be modified. For instance, consider a general deep double-well case, i.e., $N_x, N_y \gg N_1, N_2, N_3$. In such a limit, Eq. (24) reduces to the following:

$$P_{b \leftarrow a} = \frac{N_1 N_2 N_3}{N_a (N_1 N_2 + N_2 N_3 + N_3 N_1 + N_2 N_2)}, \quad (\text{A1})$$

which is different from the formula derived by Bower *et al.*⁴⁶ using a branching analysis assuming the statistical behavior of the deep double-well dynamics:

$$P_{b \leftarrow a} = \frac{N_1 N_2 N_3}{N_a (N_1 N_2 + N_2 N_3 + N_3 N_1)}. \quad (\text{A2})$$

Evidently, Eq. (A1) has the incorrect limit of vanishingly small reaction probability for the case $N_x, N_y \gg N_2 \gg N_1, N_3$.

In the following, we shall derive the correct $P_{b \leftarrow a}$ for a general double-well problem with the UST approach, and clarify the approximation inherent in Eq. (24).

In the branching analysis, the most general scenario includes the following three processes for the double-well system: trapped in the first well \mathbf{x} for n times; jump between the two wells \mathbf{x} and \mathbf{y} for l times, and trapped in the second well \mathbf{y} for m times. Accordingly, the probability for a trajectory going from \mathbf{a} to \mathbf{b} can be written as follows:

$$P_{b \leftarrow a} = \sum_{n,m,l=0}^{\infty} (P_{b \leftarrow y} \times P_{\text{trap},y}^m \times P_{y \leftarrow x} \times P_{\text{jump}}^l \times P_{\text{trap},x}^n \times P_{x \leftarrow a}) \times g(n,l,m), \quad (\text{A3})$$

where the new quantities are defined as follows:

$$P_{b \leftarrow a} = \frac{P_{b \leftarrow y} P_{y \leftarrow x} P_{x \leftarrow a}}{(1 - P_{\text{trap},x})(1 - P_{\text{trap},y})} \times \frac{1}{1 - \frac{P_{\text{jump}}}{(1 - P_{\text{trap},x})(1 - P_{\text{trap},y})}} \quad (\text{A7a})$$

$$= \frac{P_{b \leftarrow y} P_{y \leftarrow x} P_{x \leftarrow a}}{\{[1 - (1 - P_{x \leftarrow y})(1 - P_{b \leftarrow y})][1 - (1 - P_{y \leftarrow x})(1 - P_{a \leftarrow x})] - P_{\text{jump}}\}}. \quad (\text{A7b})$$

Comparing Eqs. (A7b) and (24), one sees immediately that the difference lies in the extra P_{jump} in the denominator of Eq. (A7b). Evidently, Eq. (24) is correct only if the second barrier is rate limiting which implies small P_{jump} . For a general deep well case, i.e., $N_x, N_y \gg N_1, N_2, N_3$, one may show straightforwardly that Eq. (A7b) reduces to the correct limit (A2).

¹(a) J. I. Steinfeld, J. S. Francisco, and W. L. Hase, *Chemical Kinetics and Dynamics* (Prentice-Hall, Englewood Cliffs, NJ, 1989); (b) D. G. Truhlar, B. C. Garrett, and S. J. Klippenstein, *J. Phys. Chem.* **100**, 12771 (1996).

²(a) R. G. Gilbert and S. C. Smith, *Theory of Unimolecular and Recombination reactions* (Oxford University Press, New York, 1990); (b) W. Forst, *Theory of Unimolecular Reactions* (Academic, New York, 1973); (c) T. Baer and W. L. Hase, *Unimolecular reaction dynamics: Theory and Experiments* (Oxford University Press, New York, 1996).

³(a) D. M. Wardlaw and R. A. Marcus, *Adv. Chem. Phys.* **70**, 231 (1988); (b) S. J. Klippenstein, *J. Chem. Phys.* **96**, 367 (1992); (c) S. J. Klippenstein and R. A. Marcus, *ibid.* **87**, 3410 (1987); (d) S. C. Smith, *J. Phys. Chem.* **97**, 7034 (1993).

⁴For a recent review, see for example, W. H. Miller, *Dynamics of Molecules and Chemical Reactions*, edited by R. E. Wyatt and J. Z. H. Zhang (Dekker, New York, 1996).

⁵See, for example, D. H. Zhang and J. C. Light, *J. Chem. Phys.* **106**, 551 (1997).

⁶(a) J. Qi and J. M. Bowman, *J. Chem. Phys.* **104**, 7545 (1996); (b) X. Sun, H. Wang, and W. H. Miller, *ibid.* **109**, 7064 (1998).

⁷(a) See, for example, J. C. Lorquet and B. Leyh-Nihant, *J. Phys. Chem.* **92**, 4778 (1988); (b) A. J. Marks and D. L. Thompson, *J. Chem. Phys.* **96**, 1911 (1992); (c) S. Hammes-Schiffer and J. Tully, *ibid.* **103**, 8528 (1995); (d) E. J. Heller and R. C. Brown, *ibid.* **79**, 3336 (1983); (e) G. E. Zahr, R. K. Preston, and W. H. Miller, *ibid.* **62**, 1127 (1975); (f) M. S. Topaler and D. G. Truhlar, *ibid.* **107**, 392 (1997).

⁸Q. Cui and K. Morokuma, *Theor. Chem. Acc.* (in press).

⁹A preliminary account of the present work was presented at the Faraday Discussion, 1–3 July 1998, St. Andrews, U. K. and was published in K. Morokuma, Q. Cui, and Z. Liu, *Faraday Discuss.* **110**, 71 (1998).

¹⁰(a) J. C. Keck, *Adv. Chem. Phys.* **13**, 85 (1967); (b) W. H. Miller, *J. Chem. Phys.* **61**, 1823 (1974).

¹¹For a review, see, for example, E. Pollak, in Ref. 4.

$$P_{\text{trap},x} = (1 - P_{y \leftarrow x})(1 - P_{a \leftarrow x}), \quad (\text{A4a})$$

$$P_{\text{trap},y} = (1 - P_{b \leftarrow y})(1 - P_{x \leftarrow y}), \quad (\text{A4b})$$

$$P_{\text{jump}} = P_{y \leftarrow x} P_{x \leftarrow y} (1 - P_{b \leftarrow y})(1 - P_{a \leftarrow x}). \quad (\text{A4c})$$

An important quantity in Eq. (A3) is the degeneracy factor $g(n,l,m)$, which accounts for the “degenerate” trajectories involving the same number of trapping/jumping events that undergo different sequences. The expression for $g(n,l,m)$ is straightforwardly written in terms of the binomial coefficients:

$$g(n,l,m) = \binom{n+l}{l} \times \binom{m+l}{l}. \quad (\text{A5})$$

Using the identity,

$$(1-x)^{-(l+1)} = \sum_{n=0}^{\infty} \binom{n+l}{l} x^n \quad (\text{A6})$$

the series summation in Eq. (A3) is readily carried out, which yields the following:

- ²⁴For a review, see, for example, H. Nakamura, in Ref. 4.
- ²⁵M. S. Child, *Molecular Collision Theory* (Academic, New York, 1974).
- ²⁶(a) G. Hirsch, R. J. Buenker, and C. Petrongolo, *Mol. Phys.* **70**, 835 (1990); (b) Y. Amatsu, K. Morokuma, and S. Yabushita, *J. Chem. Phys.* **94**, 4858 (1991); (c) T. Pacher, C. A. Mead, L. S. Cederbaum, and J. Koppel, *ibid.* **91**, 7057 (1989); (d) K. Ruedenberg and G. J. Atchity, *ibid.* **99**, 3799 (1993).
- ²⁷J. A. Miller and C. T. Bowman, *Prog. Energy Combust. Sci.* **15**, 287 (1989).
- ²⁸For a recent summary of experimental works, see J. W. Bozzelli, M. H. U. Karim, and A. M. Dean, *Proceedings of the sixth Toyota Conference on Turbulence and Molecular Processes in Combustion* (Elsevier, New York, 1993).
- ²⁹(a) M. R. Manaa and D. R. Yarkony, *J. Chem. Phys.* **95**, 1808 (1991); (b) *Chem. Phys. Lett.* **188**, 352 (1991).
- ³⁰J. M. L. Martin and P. R. Taylor, *Chem. Phys. Lett.* **209**, 143 (1993).
- ³¹S. P. Walch, *Chem. Phys. Lett.* **208**, 214 (1993).
- ³²(a) T. Seideman and S. P. Walch, *J. Chem. Phys.* **101**, 3656 (1994); (b) T. Seideman, *ibid.* **101**, 3662 (1994).
- ³³(a) A. S. Rodgers and G. P. Smith, *Chem. Phys. Lett.* **253**, 313 (1996); (b) J. A. Miller and S. P. Walch, *Int. J. Chem. Kinet.* **29**, 253 (1997).
- ³⁴W. H. Miller, *J. Chem. Phys.* **65**, 2216 (1976).
- ³⁵In our derivation, it is assumed that the middle "saddle point" (MSX) is the bottleneck, and therefore the effect from the recrossing of the MSX is neglected. This approximation should be reasonable given the small inter-system crossing probability for the present system. See the Appendix for details.
- ³⁶J. Qi and J. M. Bowman, *J. Chem. Phys.* **105**, 9884 (1996).
- ³⁷See, for example, (a) Q. Sun, D. L. Yang, N. S. Wang, J. M. Bowman, and M. C. Lin, *J. Chem. Phys.* **93**, 4730 (1990); (b) J. M. Bowman, *Adv. Chem. Phys.* **61**, 151 (1985); J. M. Bowman and A. F. Wagner, in *Theory of Chemical Reaction Dynamics*, edited by D. C. Clary (Reidel, Dordrecht, 1986), p. 47.
- ³⁸See, for example, E. L. Sibert III, *Int. Rev. Phys. Chem.* **9**, 1 (1990).
- ³⁹The singularity can be transformed away by rewriting the Hamiltonian as a function of $z = \cos \theta$ as shown by B. T. Stutcliffe, *Mol. Phys.*, **48**, 561 (1983).
- ⁴⁰For a recent review, see, for example, K. Anderson and B. Roos, in Ref. 15.
- ⁴¹A. M. Mebel, K. Morokuma, and M. C. Lin, *J. Chem. Phys.* **103**, 7414 (1995).
- ⁴²M. Baer and M. S. Child, *Mol. Phys.* **36**, 1449 (1978).
- ⁴³S. L. Mielke, G. J. Tawa, D. G. Truhlar, and D. W. Schwenke, *Chem. Phys. Lett.* **234**, 57 (1995).
- ⁴⁴D. G. Truhlar, *Faraday Discuss.* **110**, 521 (1998).
- ⁴⁵For a previous treatment of the N₂O system with similar spirit as the current work, see J. Tully, *J. Chem. Phys.* **61**, 61 (1974).
- ⁴⁶W. J. Chesnavich, L. Bass, T. Su, and M. T. Bowers, *J. Chem. Phys.* **74**, 2228 (1981).